

## Characterization of Acid-Base Properties of Polymers and Other Materials: Relevance to Adhesion Science and Technology

Mohamed M. Chehimi<sup>1\*</sup>, Eva Cabet-Deliry<sup>2</sup>, Ammar Azioune<sup>1</sup> and Marie-Laure Abel<sup>1#</sup>

<sup>1</sup>ITODYS, Université Paris 7 - CNRS (ESA 7086), 1 rue Guy de la Brosse, 75005 Paris, France

<sup>2</sup>Laboratoire d'Electrochimie Moléculaire, Université Paris 7 - 2 place Jussieu, 75005 Paris, France

**SUMMARY:** This paper reviews the background to the theory of Lewis acid-base (AB) interactions in adhesion, adsorption, wetting and mixing of polymers and other materials (pigments, fillers, fibres, etc.). These specific materials interactions require the revision of old concepts (« polar » interactions) and the development of new analytical techniques and methodologies. Four of the most currently used techniques to characterize AB interactions are described : contact angle measurements, inverse gas chromatography, X-ray photoelectron spectroscopy, and atomic force microscopy.

### Introduction

The reversible work of adhesion ( $W$ ) is the free energy change per unit area in creating an interface between two bodies (*e.g.* an adhesive and an adherend). It is related to the interfacial molecular forces. However,  $W$  may be obscured by other factors (*e.g.* mechanical interlocking, interdiffusion) since it is a few orders of magnitude lower than the measured adhesive joint strength<sup>[1]</sup>. One important contribution to practical adhesion is the energy loss due to irreversible deformation processes within the adhesive. Nevertheless, viscoelastic losses were found to be proportional to  $W$ <sup>[2]</sup>. For this reason, it is important to determine the nature of interfacial chemical and physical forces and to understand how they control adhesion.

In recent years it has become clear that acid-base interactions (AB) promote adsorption, wetting, adhesion and mixing<sup>[3,4]</sup>. The knowledge of the AB properties of polymers, fibres and fillers is an important step towards the design of high performance materials (*e.g.* composites, coatings and

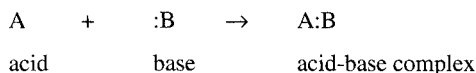
---

\* present address : School of Mechanical and Materials Engineering, University of Surrey, Guildford, UK

blends). The durability of such materials relies to a great extent on adhesion. Although adhesion can be good without any pretreatment, in several practical situations it was conclusively shown that pretreatments of fibres or metal oxides were necessary and required surface grafting of functional groups with appropriate acidity and/or basicity for a good and durable adhesion. The aim of this paper is (i) to review the role of AB interactions in adhesion, and (ii) to describe the use of contact angle measurements (CAM), inverse gas chromatography (IGC), X-ray photoelectron spectroscopy (XPS) and atomic force microscopy (AFM) in this regard.

## Definition, Properties and Strength of Acid-base Interactions

AB interactions, including hydrogen bonds, are specific; they are not ubiquitous like dispersive interactions. They occur when a base and an acid are brought close together :



Acids can be  $n$ ,  $\sigma^*$  and  $\pi^*$  electron acceptors; and bases  $n$ ,  $\sigma$  and  $\pi$  electron donors. Hydrogen or AB bonds are exothermic (8-50 kJ/mol). The positive or the negligibly small negative entropic term  $-T\Delta S$  is overcome, so that adhesion and wetting can be substantially improved. The high energy associated with AB interactions is due to short range (2-3 Å) Coulombic forces. The heat of AB adduct formation can be determined using Drago's equation<sup>[5]</sup> <sup>1</sup>:

$$-\Delta H^{AB} = (E_A \cdot E_B + C_A \cdot C_B) \quad (1)$$

Alternatively, Gutmann<sup>[6]</sup> proposed a two-parameter equation for the estimation of  $\Delta H^{AB}$  <sup>1</sup>:

$$-\Delta H^{AB} \text{ (kcal/mol)} = (AN \cdot DN)/100 \quad (2)$$

Lewis AB interactions account for the high boiling point and surface tension of water, and the double helical structure of DNA. They affect polymer glass transition temperature and miscibility<sup>[8]</sup>, swelling and solubility<sup>[9]</sup>, adsorption and adhesion<sup>[3,4]</sup>.

<sup>1</sup> In (1),  $E$  and  $C$  are the susceptibilities of the acid (A) and the base (B) to undergo an electrostatic interaction (E) and a covalent bond (C), respectively.  $\Delta H^{AB}$  can be determined using (1) with an accuracy of 0.4-0.8 kJ/mol.

## Theory of Acid-base Interactions in Adhesion

In the absence of chemisorption and interdiffusion,  $W$  is expressed by Dupré's equation :

$$W = \gamma_1 + \gamma_2 - \gamma_{12} \quad (3)$$

where  $\gamma_i$  is the surface free energy of component  $i$  and  $\gamma_{12}$  is the interfacial free energy.  $W$  and  $\gamma$  have additive components ( $W = W^d + W^p + W^{AB} + W^m$ ; and  $\gamma = \gamma^d + \gamma^p + \gamma^{AB} + \gamma^m$ ) due to dispersive (d), dipolar (p), acid-base (AB) and metallic bonding (m)<sup>[10]</sup>. For this reason, it is important to determine the nature of the forces operating at interfaces and their effects on adhesion.

For two materials interacting via London dispersive forces only, it was suggested<sup>[10]</sup> that :

$$W = W^d = 2(\gamma_1^d \cdot \gamma_2^d)^{1/2} \quad (4)$$

If material 1 is acidic (basic) and material 2 basic (acidic), they can interact via AB forces, thus :

$$W = W^d + W^{AB} \quad (5)$$

where  $W^{AB}$  is the AB contribution to  $W$ . van Oss *et al.*<sup>[11]</sup> introduced the notion of acidic and basic components to the surface energy ( $\gamma^+$  and  $\gamma^-$ , respectively) of materials to estimate  $W^{AB}$  :

$$W^{AB} = 2(\gamma_1^+ \gamma_2^-)^{1/2} + 2(\gamma_1^- \gamma_2^+)^{1/2} \quad (6)$$

The total AB contribution to the surface free energy is :  $\gamma^{AB} = 2(\gamma^+ \gamma^-)^{1/2}$ . For liquids,  $\gamma_L^+$  and  $\gamma_L^-$  were established on the assumption that for water  $\gamma_L^- = \gamma_L^+ = 25.5 \text{ mJ/m}^2$ .

Equation (6) is much more reliable than the equation of Owens and Wendt<sup>[12]</sup> <sup>2</sup> in rationalizing non-dispersive interactions of polymers. The approach of Owens and Wendt actually fails to predict, for example, the miscibility of a water-ethanol system<sup>[7]</sup> and the solubility of PEO in water<sup>[13]</sup>.

## Experimental Study of Acid-base Properties of Polymers and other Materials

Several analytical techniques and methodologies have been established to assess the AB properties of materials.<sup>[3,4]</sup> The focus of this paper will be on the use of Contact Angle Measurements (CAM), Inverse Gas Chromatography (IGC), X-ray Photoelectron Spectroscopy (XPS) and Atomic Force Microscopy AFM.

<sup>1</sup> In (2), AN is the acceptor number of the acidic species and DN the donor number of the basic species.  $DN = -\Delta H(\text{SbCl}_5/\text{base})$ , determined in 1,2-dichloroethane, AN : relative <sup>31</sup>P NMR shift of triethylphosphine oxide dissolved in the candidate acid. AN values have been corrected for dispersive (d) interactions and in the new scale,  $AN^* = 0.228(AN - AN^d)$  in kcal/mol<sup>[7]</sup>.

<sup>2</sup>  $W = 2(\gamma_1^d \cdot \gamma_2^d)^{1/2} = 2(\gamma_1^p \cdot \gamma_2^p)^{1/2}$ , the so-called "extended Fowkes method" by analogy to (4).

## 1. Contact Angle Measurements

### 1.1. Determination of the Surface Tension Components

The wetting of a solid surface by a liquid drop (Figure 1) is expressed by Young's equation :

$$\gamma_s - \gamma_{SL} = \gamma \cos \theta \quad (7)$$

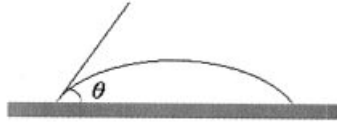


Fig. 1: Contact angle of a liquid wetting a polymer surface.

Combination of (3) and (7) leads to the Young-Dupré's equation of the work of adhesion :

$$W_a = \gamma_L(1 + \cos \theta) = 2(\gamma_s^d \gamma_L^d)^{1/2} + 2(\gamma_s^+ \gamma_L^-)^{1/2} + 2(\gamma_s^- \gamma_L^+)^{1/2} \quad (8)$$

Using at least three test liquids of known surface tension components one determines  $\gamma_s^d$ ,  $\gamma_s^+$  and  $\gamma_s^-$  for the material under test and hence the total surface free energy  $\gamma_s = \gamma_s^d + 2(\gamma_s^+ \gamma_s^-)^{1/2}$ .

It is important to note that the unknowns  $(\gamma_s^+)^{1/2}$  and  $(\gamma_s^-)^{1/2}$  in (8) must be positive.

Table 1 tabulates the surface tension components for selected liquids, polymers and other materials. There are some interesting points about the  $\gamma^+$  and the  $\gamma^-$  values:

- (i) PEO is a fairly basic polymer, more so than methacrylate polymers.
- (ii)  $N_2$  plasma significantly increases the basicity of a PP surface due to the grafted amine groups.
- (iii) Conducting polypyrrole is fairly acidic due to the pyrrole units and the positively charged chains.
- (iv) APS-treated glass is very basic due to the surface amino groups. For Glass-C18,  $\gamma \approx \gamma_s^d$  and the AB character is weak due to a quasi total screening of glass surface by the hydrophobic octadecylsilane.
- (v) The basicity of HSA is due to the peptide linkages.

Table 1: Surface tension components (in mJ/m<sup>2</sup>) for selected polymers and other materials.

Materials	$\gamma$	$\gamma^d$	$\gamma^{AB}$	$\gamma^+$	$\gamma^-$	Ref.
Water	72.8	21.8	51	25.5	25.5	14
Glycerol	64	34	30	3.92	57.4	14
Formamide	58	39	19	2.28	39.6	14
CH <sub>2</sub> I <sub>2</sub>	50.8	50.8	0	0	0	14
PEO 6000	43	43	0	0	64	13
PMMA	39-43	39-43	0	0	9.5-22.4	14
PVC	43.7	43	0.7	0.04	3.5	14
PPyTS	47.0	41.0	6.0	0.81	10.9	15
PPyDS	41.7	34.8	6.9	1.35	8.85	15
PPyCl	43.5	36.6	6.9	0.43	28.3	15
Untreated PP	32.2	30.1	2.1	0.3	3.8	16
N <sub>2</sub> plasma-treated PP	53.3	41.9	11.4	1.0	30.9	16
HSA, dry, pH 7	41.4	41.0	0.4	0.002	20	17
Glass	59.3	42.03	17.80	1.97	40.22	18
Glass-C18	26.8	25.70	1.12	0.24	1.32	18
Glass-APS	45.0	39.2	5.76	0.084	98.62	15

HSA : human serum albumin ; PPyTS: tosylate-doped polypyrrole; PPyDS: dodecyl sulfate-doped polypyrrole; PPyCl: chloride-doped polypyrrole; glass-APS: aminopropylsilane-treated glass.

### 1.2. Interfacial Protein-Polypyrrole Interaction Energies

HSA was adsorbed onto PPyCl, PPyDS and PPyTS powders<sup>[15]</sup> from buffered medium at pH 7.4. The PPy-HSA (*I-2*) interaction in water (*w*) is expressed by :  $\Delta G_{1W2} = \gamma_{12} - \gamma_{1W} - \gamma_{2W}$ ; where  $\gamma_{ij}$  is the interfacial tension between materials *i* and *j*. Using the VOGC theory<sup>[17]</sup>,  $\Delta G_{1W2}$  is rewritten as:

$$\Delta G_{1W2} = (\sqrt{\gamma_1^d} - \sqrt{\gamma_2^d})^2 - (\sqrt{\gamma_1^d} - \sqrt{\gamma_w^d})^2 - (\sqrt{\gamma_2^d} - \sqrt{\gamma_w^d})^2 + 2[\sqrt{\gamma_w^+} (\sqrt{\gamma_1^-} + \sqrt{\gamma_2^-} - \sqrt{\gamma_w^-}) + \sqrt{\gamma_w^-} (\sqrt{\gamma_1^+} + \sqrt{\gamma_2^+} - \sqrt{\gamma_w^+}) - \sqrt{\gamma_1^-} \gamma_2^+ - \sqrt{\gamma_1^+} \gamma_2^-] \quad (9)$$

(9) permits the calculation of  $\Delta G_{1W2}$  and its dispersive and acid-base contributions (Table 2).

Table 2: Adsorption (mg/g) and interfacial interaction energies (mJ/m<sup>2</sup>) for HSA and polypyrroles immersed in water.

Support	Adsorption (mg/g)	$\Delta G_{1W2}$	$\Delta G_{1W2}^d$	$\Delta G_{1W2}^{AB}$
PpyCl	27±2.5	-7.6	-4.8	-2.8
PpyDS	40±5	-29.6	-4.3	-25.3
PpyTS	70±10	-46	-3.3	-42.7

The negative  $\Delta G_{1W2}$  values indicate that the hydrophobic PPy-HSA interaction is attractive.  $\Delta G_{1W2}$  values parallel the trends of HSA adsorption. More importantly, there is a strong supporting evidence for the important role of AB interactions in HSA adsorption onto polypyrroles.

The VOGC theory has been used elsewhere to study polymer solubility<sup>[13]</sup>, protein adsorption on clays<sup>[17]</sup>, cell adhesion<sup>[19]</sup>, fibre-matrix adhesion<sup>[20]</sup> and glass-colloid (de)adhesion<sup>[18]</sup>.

### 1.3. Contact Angle Titration (CAT)

CAT is a method for studying surfaces with Brönsted AB chemistry. Contact angles are measured for aqueous solutions of given pHs. For pH = 0-14,  $\gamma_L$  is pH-independent and equals that of distilled water. The CAT data result in a titration curve with the highest value of W obtained for low (high) pH solutions in contact with basic (acidic) surfaces. CAT has been applied to study PBAC and polyethersulfone<sup>[21]</sup>, silica and carbon fibres<sup>[21]</sup>, NH<sub>3</sub> and O<sub>2</sub> plasma-treated PP<sup>[22]</sup>, surface COOH-functionalized PE<sup>[23]</sup>; and to estimate the IEPs of metal oxides<sup>[24]</sup>

## 2. Inverse Gas Chromatography (IGC)

IGC is widely used to characterize polymers, fillers, pigments and fibres over a wide temperature range. The term "inverse" means that the stationary phase is of interest, in contrast to conventional GC. At infinite dilution,  $-\Delta G_a = RT \ln(V_N) + C$ ; where  $\Delta G_a$  is the free energy of adsorption, R is the gas constant, T the column temperature,  $V_N$  the retention volume, and C a constant.  $V_N$  data treatment is a key to the study of dispersive and AB properties of materials. N-alkanes are used to determine the dispersive properties of materials, and reference Lewis acids

and bases probe the basic and acidic properties, respectively. Figure 2 depicts plots of  $\Delta G_a$  or  $RT\ln(V_N)$  values vs. the number of carbon atoms in the n-alkane series for PPyNO<sub>3</sub> powder, PMMA/PVC blend-coated PPyNO<sub>3</sub> (PPy/PMMA/PVC) and PMMA. The slope of each plot is equivalent to  $\Delta G^{CH_2}$ , since there is a CH<sub>2</sub> increment between two successive n-alkanes. According to Dorris and Gray<sup>[25]</sup>:

$$\gamma_s^d = (1/4 \gamma_{CH_2}) \times (\Delta G_a^{CH_2} / N a_{CH_2})^2$$

where  $\gamma_{CH_2}$  is the surface tension of a methylene group ( $\gamma_{CH_2}(\text{mJ/m}^2) = 36.8 - 0.058.T(^{\circ}\text{C})$ ), N the Avogadro number and  $a_{CH_2}$  the surface area of a CH<sub>2</sub> group.

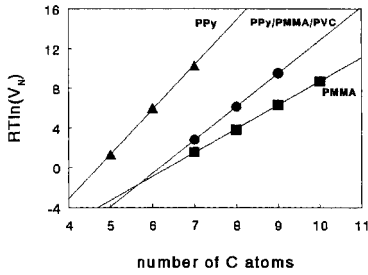


Fig. 2:  $RT\ln(V_N)$  vs the number of carbon atoms in the n-alkane series adsorbed on PPyNO<sub>3</sub>, PPy/PMMA/PVC and PMMA at 48 °C.

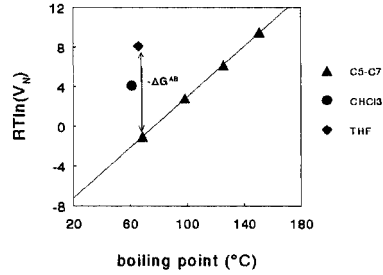


Fig. 3:  $RT\ln(V_N)$  vs the boiling point for probes adsorbed onto PPy/PMMA/PVC.

In the case of solid-probe AB interactions,  $\Delta G_a = \Delta G_a^d + \Delta G_a^{AB}$ .  $\Delta G_a^{AB}$  is subtracted using :

$$-\Delta G_a^{AB} = -(\Delta G_a - \Delta G_a^d) = RT\ln(V_N/V_{N,ref}) \quad (10)$$

where  $V_{N,ref}$  is the net retention volume of a hypothetical reference n-alkane having the same molecular descriptor. Figure 3 shows a plot of  $RT\ln(V_N)$  vs the boiling point for n-alkanes, THF and CHCl<sub>3</sub> adsorbed onto PPy/PMMA/PVC. The n-alkanes yield a reference line defining the dispersive interactions for the adsorbent-probe pairs. For probes interacting via AB forces, the vertical distance between the respective markers and the reference line accounts for  $\Delta G_a^{AB}$ .

There are several methods which permit to determine AB descriptors.<sup>[15]</sup> A simple method involves relating  $-\Delta G_a^{AB}$  to Gutmann's constants of the probes :

$$-\Delta G^{AB} = RT \ln(V_N/V_{N,\text{ref}}) = DN \cdot K_A + AN^* \cdot K_B \quad (11)$$

where  $K_A$  and  $K_B$  are the acidity and basicity constants to be determined for the tested material. Graphically, a plot of  $[RT \ln(V_N/V_{N,\text{ref}})]/AN^*$  versus  $DN/AN^*$  leads to a linear correlation of which slope and intercept are equal to  $K_A$  and  $K_B$ , respectively.

Table 3 shows the dispersive and AB properties of PPy/PMMA/PVC materials and their reference polymers (PPyNO<sub>3</sub>, PMMA and PVC), recorded separately.

Table 3:  $\gamma_s^d$  values and  $K_A$  and  $K_B$  constants for PPyNO<sub>3</sub>, PVC, PMMA and PMMA/PVC blend-coated PPyNO<sub>3</sub> (data at 48 °C).

Materials	$\gamma_s^d$ (mJ/m <sup>2</sup> )	$K_A$	$K_B$	$K_A/K_B$
PPyNO <sub>3</sub>	113	11.5	19.2	0.6
PVC	31	14.9	21.8	0.68
PMMA	40	7.6	35.4	0.21
PMMA/PVC blend-coated PPyNO <sub>3</sub>	48-63	10.1-11.5	24.4-29.2	0.38-0.43

PMMA and PVC were coated onto PPyNO<sub>3</sub> from THF or dioxane. Initial concentrations of PMMA/PVC in g/l were 0.88/0.88, 1.56/0.88 and 2.64/0.88.  $K_A$  and  $K_B$  were determined using CHCl<sub>3</sub> ( $DN = 0$  kJ/mol,  $AN^* = 22.6$  kJ/mol) and THF ( $DN = 83.7$  kJ/mol ;  $AN^* = 2.1$  kJ/mol), acidic and amphoteric probes, respectively.

$\gamma_s^d$  values for PPy/PMMA/PVC lie in the 48-63 mJ/m<sup>2</sup> range, which is intermediate between the values determined for the substrate (PPyNO<sub>3</sub>) and the adsorbates (PVC and PMMA). These intermediate  $\gamma_s^d$  values suggest that the adsorbed blend is patchy. The relative basicity decreased in the order PMMA > blend coated-PPy > PVC and PPy, which suggests that the blend patches have a PMMA rich-surface (see Figure 4). Thus the PPy-blend interface is PVC-rich.

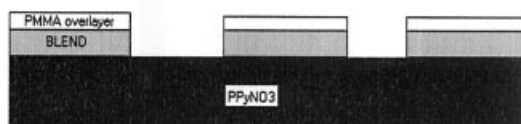


Fig. 4: Illustration of a polypyrrole surface partially coated with a PMMA/PVC blend.



IGC-derived AB descriptors were also very useful for interpreting the interfacial shear resistance of carbon fibre composites or the adsorption of dispersion and binder resins onto pigments<sup>[15]</sup>.

### 3. X-ray Photoelectron Spectroscopy (XPS)

XPS has been used in adhesion science to study the locus of failure of adhesive joints and identifying molecular species segregating at polymer-metal interface.<sup>[26]</sup> It is also a means of determining IEPs of metal oxides and AB properties of catalysts and organic molecules.<sup>[15]</sup>

As far as polymers are concerned, Chehimi *et al*<sup>[27]</sup> proposed to estimate their AB properties using adsorbed molecular probes. If the polymer-solute interaction is strong enough (*e.g.* via AB forces) then a residual amount of solute is detected.  $\text{CHCl}_3$ ,  $\text{CH}_2\text{Cl}_2$ , hexafluoroisopropanol (HFIP),  $\text{CF}_3\text{COOH}$ ,  $\text{I}_2$  and pyrrole probe Lewis basicity, whereas pyridine and DMSO are suitable to study surface acidity. Established with homopolymers such as PMMA, this method was further applied to plasma-treated polypropylene. Figure 5 depicts survey scans of PP and ammonia plasma treatment (APTPP) after exposure to  $\text{CHCl}_3$ . The retention of the solute is due to favourable AB interactions with the surface-grafted amino groups. In contrast, PP undergoes weak dispersive interactions with the solute, which cannot tolerate the ultra-high vacuum.

The uptake of  $\text{CHCl}_3$  by PP surfaces ( $\text{CHCl}_3/\text{N}$  molar ratio) versus the treatment time is depicted in Figure 6. A plateau value is readily reached at molar ratio (5-6 %) and optimal time is around 1 s. With longer treatment time,  $\text{CHCl}_3$  uptake decreases sharply. The variation in the  $\text{CHCl}_3/\text{N}$  ratio vs treatment time correlated with the adhesion of vapor-deposited aluminium to APTPP, thus suggesting that metal-polymer adhesion strongly depended on interfacial AB interactions.

Evidence for the AB interactions was provided by the chemical shifts of the  $\text{Cl}2\text{p}$  core level :  $\text{CHCl}_3$  undergoes negative shifts (lower  $\text{Cl}2\text{p}$  binding energy, BE) when it is adsorbed on a basic surface. Indeed, a Lewis acid is an electron acceptor and upon interaction with a base electron density is transferred to the former, thus yielding a lower BE. The opposite reasoning holds for basic probes.

For a series of polymer- $\text{CHCl}_3$  pairs, the following relationship has been established<sup>[27]</sup> :

$$-\Delta H^{\text{AB}}(\text{kcal.mol}^{-1}) = 228.8 - 1.14\text{BE}(\text{eV}) \quad (12)$$

This equation permits the estimation of  $\Delta H^{AB}$  values for APTPP- $\text{CHCl}_3$  pairs. The results compared favourably with the  $\Delta H^{AB}$  calculated using Drago's equation for amine- $\text{CHCl}_3$  adducts.<sup>[27]</sup> Equation (12) has also been used to derive Drago's E and C constants for PPO.<sup>[27]</sup>

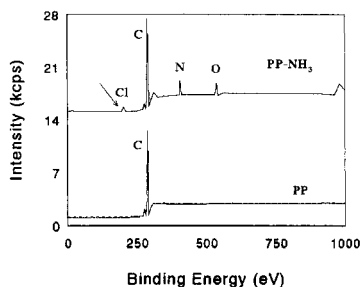


Fig. 5: Survey scans of untreated PP and 0.7 s APTPP after exposure to  $\text{CHCl}_3$  vapours.

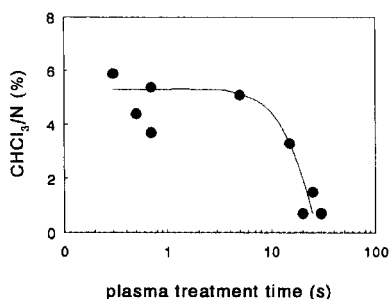


Fig. 6: Chloroform to nitrogen molar ratio (in %) vs the ammonia plasma treatment time of PP.

#### 4. Atomic Force Microscopy (AFM)

In adhesion, the manifestations of AB interactions have been observed at the macroscopic and microscopic scales (wetting, adhesion, etc.). The development of AFM over the last decade has led to the possibility of measuring adhesion forces on at the molecular scale, in addition to imaging surfaces in atomic resolution. The attractive and repulsive forces between the tip of and the surface include van der Waals interactions, hydrogen bonds, capillary action, or electrostatic fields. When the tip is brought near the surface it may jump into contact in the case of sufficient attractive forces. Once in contact, repulsive forces lead to deflection of the cantilever in the opposite direction. On withdrawal, adhesion during contact may cause the cantilever to adhere to the sample some distance past the initial contact. The tip comes free from the surface at a point where adhesion is broken. The force ( $F$ ) required to break adhesion is a key parameter of the AFM force curve.

Figure 7 depicts force-vs-distance curves obtained for a colloidal silica-modified tip and COOH-terminated thiol-modified gold substrates. For silica-COOH interactions, the force-vs-distance curves indicate that below pH 6-6.3 the interaction is purely attractive because the terminal COOH groups are not ionized.<sup>[28]</sup> At higher pH, repulsive forces operate at the tip-COO<sup>-</sup> interface. The surface potential of the specimens can be derived from  $F/R$ -vs-distance curves ( $R$  being the tip radius) and related to pH as shown in Figure 8. The surface potential of the surface-confined COOH groups is clearly pH-dependent. Since the surface potential is directly related to the fractional degree of surface carboxylic acid dissociation, one can thus view the plot in Figure 8 as a direct surface acid titration curve. The apparent  $pK_a$  of the adsorbed COOH corresponds to the inflection point of the sigmoidal plot, near pH 8.0. This is a much higher value (about 3.5 units) than the  $pK_a$  measured for similar acids in bulk aqueous solution. This is due to strong lateral hydrogen bonding between the confined COOH groups.<sup>[28]</sup>

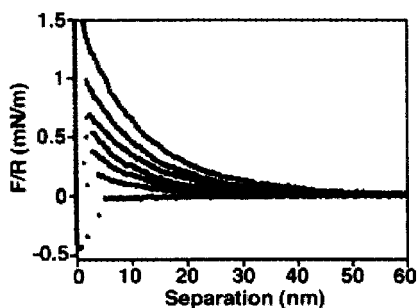


Fig. 7 : Force between silica probe and COOH-terminated thiol-covered gold in 0.1 M KCl vs pH. Curves correspond to pH 6, 7, 7.5, 8, 8.5 and 9 from bottom to top (reprinted with permission from ACS).

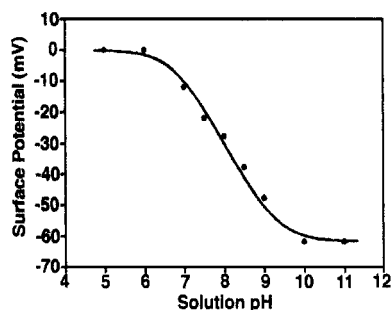


Fig. 8 : Measured (●) and theoretical (—) surface potentials of the COOH groups in 0.1 M KCl vs pH. The inflection point corresponds to  $pK_a$  (reprinted with permission from ACS).

Several other AB studies involved mercaptan-functionalized tips and surfaces.<sup>[29,30]</sup> Titration curves were, obtained, for example for carboxylic acid, phosphonic acid and amino groups.<sup>[30]</sup> In the case of  $PO_3H_2$ -functionalized tip and  $PO_3H_2$ -functionalized surface, adhesion force-vs-pH

plot exhibited two inflection points corresponding to the ionization steps  $\text{PO}_3\text{H}_2 \rightarrow \text{PO}_3\text{H}^-$  and  $\text{PO}_3\text{H}^- \rightarrow \text{PO}_3^{2-}$ . These peculiar points correspond to  $\text{pK}_a$  values of 4.7 and 11.6, respectively.

Thomas *et al.*<sup>[29]</sup> estimated the work of adhesion for various combinations ( $\text{CH}_3$ -vs- $\text{CH}_3$ ,  $\text{NH}_2$ -vs- $\text{NH}_2$ ,  $\text{COOH}$ -vs- $\text{COOH}$  and  $\text{NH}_2$ -vs- $\text{COOH}$ ) using  $W = F/2\pi R$  and found the  $\text{NH}_2$ -vs- $\text{COOH}$  interaction large and negative, with a bond energy of 67 kJ/mol.

## Conclusion

It has been shown in this paper that Lewis acid-base interactions play an important role in interfacial phenomena such as adsorption, wetting, adhesion and mixing. The importance of such findings by the "adhesion community" resulted in the establishment of an impressive array of methods, which enable us to derive acid-base scales for polymers and other materials. Whilst contact angle measurements and inverse gas chromatography continue to be essential techniques to study acid-base interactions, XPS has proved to be versatile and applicable to both polymers and metal oxides in a variety of approaches. Finally, AFM has become a very powerful tool with which to study acid-base forces on the molecular scale. AFM confirmed that functional groups confined to surfaces have acid-base properties that differ markedly from those in a bulk solution. It is hoped, however, that Round Tables will be organised in order to define common strategies for the characterization of acid-base properties of polymers and other materials. This will lead to more consistency in the results and make inter-laboratory comparison possible.

## References

1. A. J. Kinloch, *J. Mater. Sci.*, **1980**, 15, 2141
2. A. N. Gent, J. Schultz, *J. Adhesion* **1972**, 3, 281
3. K.L. Mittal, H.R. Anderson, Jr., "*Acid-Base Interactions: Relevance to Adhesion Science and Technology*", VSP, Utrecht 1991
4. K. L. Mittal, "*Acid-Base Interactions. Relevance to Adhesion Science and Technology, vol. 2*", VSP (Utrecht, The Netherlands), 2000.
5. R. S. Drago, *Structure and Bonding*, **1973**, 15, 73
6. V. Gutmann, "*The Donor-Acceptor Approach to Molecular Interactions*", Plenum Press, New York, 1978
7. F. M. Fowkes, *J. Adhesion Sci. Technol.*, **1990**, 4, 669
8. A. A. Lin, T. K. Kwei and A. Reiser, *Macromolecules*, **1989**, 22, 4112
9. F. M. Fowkes, D. O. Tischler, J. A. Wolfe, L. A. Lannigan, C. M. Ademu-John, M. J. Halliwell, *J. Polym. Sci., Chem. Ed.*, **1984**, 22, 547
10. F. M. Fowkes, *Ind. Eng. Chem.*, **1964**, 56 (112), 40
11. C. J. van Oss, R. J. Good, M. K. Chaudhury, *Langmuir*, **1988**, 4, 884
12. D. K. Owens and R. C. Wendt, *J. Appl. Polym. Sci.*, **1969**, 13, 1741
13. C. J. van Oss, R. J. Good, *Langmuir*, **1992**, 8, 2877

14. R. J. Good, M. K. Chaudhury, C. J. van Oss, in "Fundamentals of Adhesion", L.-H. Lee (Ed.), Plenum Press, New York 1991. chap. 4
15. M. M. Chehimi, A. Azioune, E. Cabet-Deliry, in "Handbook of Adhesive Technology", K. L. Mittal and A. Pizzi (Eds.), Marcel Dekker Inc. (NY), in press
16. F. Bodino, PhD Thesis, Facultés Universitaires Notre-Dame de la Paix (Namur, Belgium), **1998**, p. 143
17. P. M. Costanzo, R. F. Giese, C. J. van Oss, *J. Adhesion Sci. Technol.*, **1990**, *4*, 267
18. A. M. Freitas, M. M. Shasma, *Langmuir*, **1999**, *15*, 2466
19. K. W. Millsap, R. Bos, H. J. Busscher H. C. van der Mei, *J. Colloid Interface Sci*, **1999**, *212*, 495
20. N. Dilsiz, J. P. Whightman, *Colloids Surf. A*, **2000**, *164*, 325
21. K. J. Hüttinger, S. Höhmann-Wien, G. Krekel, *J. Adhesion Sci. Technol.*, **1992**, *6*, 317
22. F. Arefi-Khonsari, M. Tatoulian, N. Shahidzadeh, M. M. Chehimi, J. Amouroux, D. Leonard, P. Bertrand, in "Adhesion Science and Technology", (W. J. van Ooij and H. R. Anderson, Jr., Eds.), VSP, Utrecht, The Netherlands (1998), pp. 329-353
23. G. M. Whitesides, H. A. Biebuyck, J. P. Folkers, K. L. Prime in ref. [3], pp. 229-241
24. E. McCafferty, J. P. Whightman, *J. Adhesion Sci. Technol.*, **1999**, *13*, 1415
25. G.M. Dorris, D.G. Gray, *J. Colloid Interface Sci.*, **1980**, *77*, 353
26. J. F. Watts, in "Handbook of Surface and Interface Analysis", J. C. Rivière and S. Myhra (Eds.), Marcel Dekker Inc. (NY), chap. 18
27. M. M. Chehimi, M. Delamar, J. Kurdi, F. Arefi-Khonsari, V. Lavaste, J. F. Watts, in ref. [4], pp. 275-298
28. K. Hu, A. J. Bard, *Langmuir*, **1997**, *13*, 5114
29. R. C. Thomas, J. E. Houston, R. M. Crooks, T. Kim, T. A. Michalske, *J. Am. Chem. Soc.*, **1995**, *117*, 3830
30. E. W. van der Vegte, d G. Hadzioannou, *J. Phys. Chem. B*, **1997**, *101*, 9563

